Chemical Physics 422 (2013) 195–203

Contents lists available at SciVerse ScienceDirect

Chemical Physics

journal homepage: www.elsevier.com/locate/chemphys

Electronic spectroscopy of lumiflavin in superfluid helium nanodroplets

Alexander Vdovin [a,b], Alkwin Slenczka [a], Bernhard Dick [a,*]

[a] Institut für Physikalische and Theoretische Chemie, Universität Regensburg, 93053 Regensburg, Germany
[b] Philips Research, High Tech Campus 34, 5656 Eindhoven, The Netherlands

ARTICLE INFO

Article history:
Available online 16 November 2012

Keywords:
He droplets
Lumiflavin
High resolution spectroscopy
Vibrational structure
Electronically excited state

ABSTRACT

We present the fluorescence excitation and dispersed emission spectra of lumiflavin doped into superfluid He nanodroplets. Both spectra show well resolved vibrational structure. The electronic origin transition at 21511 cm^{-1} is the strongest line in both spectra. Quantum chemical calculations with DFT and CASSCF methods support the assignment of S_1 to a $\pi\pi^*$ excited state. We obtain vibrational frequencies in the ground and lowest excited singlet state that can serve to test the validity of quantum chemical calculations. Multidimensional Franck–Condon factors are in good agreement with the intensities within the vibrational structure for S_0 and S_1. The strongest progression forming mode has a frequency of 164 cm^{-1} in both states and is assigned to an in-plane bending mode of the whole flavin chromophore with a large amplitude on the two methyl groups at ring I.

1. Introduction

Flavins are essential protein cofactors in all living cells. The most common examples are riboflavin (RF), flavin mononucleotide (FMN) and flavin adenosine dinucleotide (FAD). Flavins can exist in several protonation states and redox states, and are hence ubiquitous in enzymes catalyzing redox reactions. The first absorption band of flavins is in the range $\lambda < 470$ nm, and hence flavins absorb blue light. Nature has made use of this by employing flavins in photoreceptors for blue light. Three classes of protein domains with this function have been discovered and studied during the last decade [1]: LOV (light oxygen voltage) domains [2–4], BLUF (blue light sensing using flavin) domains [5,6], and cryptochromes [7,8]. The redox properties of the electronically excited state are used in photolyase [9,10] which repairs DNA damaged by cycloadditions between adjacent bases.

Whereas optical spectroscopy can be used to follow the various electronic states during the photocycles of these flavoproteins, the study of the dynamics inside these electronic states and the interaction with the protein require often techniques that provide more local and specific information. Vibrational spectroscopy is one of the most promising techniques for this purpose. Therefore, in addition to difference infrared (IR) and Raman spectroscopy on electronic ground state species also transient spectroscopy has been employed to follow the dynamics in the electronically excited singlet and triplet states [11]. In this context demand for a theoretical description is growing, not only for an assignment of various vibrational frequencies to normal modes, but also of the effect of solvent and protein interaction on these modes and frequencies [12,13]. The reference state for most theoretical techniques is the isolated molecule in the gas phase.

So far, no vibrationally resolved gas phase spectrum of an electronic transition of a flavin has been published. The only high resolution spectrum that we could find is that of N_3-undecyllumiflavin isolated in a n-decane Shpolskii matrix at 4.2 K, published by Platenkamp et al. [14] in 1980. This study finds, on top of a broad background, several distinct sites with sharp lines. One of these sites with origin at 20956 cm^{-1} was studied by site selective excitation and fluorescence spectroscopy. The vibronic transition frequencies were compared to IR and Raman data, but no assignment was given. Although this study has been performed at high spectral resolution and at low temperature, a rigid alkane matrix is still a crude approximation of the non-interacting molecule in gas phase. The main aim of the present study was hence to obtain high resolution spectra of flavin under conditions that are as close as possible to those of the isolated molecule in the gas phase. This should establish whether the lowest excited singlet state has $\pi\pi^*$ character or, as some calculations predict, $n\pi^*$ character. As a result of our study we obtain vibrational frequencies in the ground and lowest excited singlet state that can serve to test the validity of quantum chemical calculations.

The essential optical chromophore common to riboflavin, FMN, and FAD is lumiflavin. In lumiflavin, the ribityl chain of riboflavin has been replaced by a methyl group. Further simplification by replacement of this methyl group through a hydrogen atom is not possible, since the resulting lumichrome molecule exists in a different tautomer. Ideally, one should study lumiflavin in a supersonic jet. However, at the temperature required to produce a substantial vapor pressure (ca. 1. mbar), lumiflavine will decompose

* Corresponding author.
E-mail address: bernhard.dick@chemie.uni-regensburg.de (B. Dick).

0301-0104/$ - see front matter © 2012 Elsevier B.V. All rights reserved.
http://dx.doi.org/10.1016/j.chemphys.2012.11.001

very quickly. In recent years, spectroscopy in superfluid He nanodroplets has been developed as an alternative which in many respects simulates spectroscopy in the gas phase [15,16]. He droplets of several thousand atoms are produced by expansion of helium gas at high pressure (ca. 20 bar) through a nozzle cooled to ca. 10 K. By evaporation from the surface these helium droplets cool to a temperature of ca. 370 mK [15]. It has been shown that He in these droplets is in the superfluid phase. Molecules can be incorporated into these droplets by collision and are subsequently cooled to the same temperature as the droplet. The vapor pressure required scales inversely with the length of the pick-up cell and is typically 10^{-4} mbar, i.e. several orders of magnitude smaller than needed for supersonic jets. Of all possible solvents liquid helium has the smallest interaction energy with dissolved molecules. This results in small shifts of the electronic transition energies with respect to the gas phase, typically less than 1 % of the transition energy [16]. Hence, He droplets could be considered as a "vacuum with high thermal conductivity". Fluorescence excitation spectra and dispersed emission spectra of large rigid organic molecules doped into He droplets show very sharp lines, even narrower than those observed in supersonic jets. Recent experiments have shown that the interaction of the molecule with the He environment is not always negligible, in particular when torsional motions are excited or substantial charge redistribution occurs upon electronic excitation. However, since other alternatives do not seem to exist, we decided to try superfluid helium droplets as a medium to study the spectra of lumiflavin under almost gaslike conditions.

2. Experiment and methods

Lumiflavin (LF) was purchased from Sigma–Aldrich corporation and used without further purification. The experimental setup for the embedding of molecules inside superfluid helium nanodroplets and their fluorescence and excitation spectroscopy was described previously [17,18]. Briefly, a continuous droplet beam was formed by supersonic expansion of pre-cooled helium at 12.5 K through a 5 μm nozzle at 20 bar stagnation pressure into a vacuum chamber. Under these conditions the average droplet has a diameter of 100 Å and contains ca. 2×10^4 helium atoms [15]. The droplets were doped with individual molecules by passing the droplet beam through a 2 cm long pick-up cell filled with LF and situated on the beam axis, heated to 210 °C. This temperature is well below the melting point of LF (325 °C [19]). The presence of the sample in the droplets was monitored with a mass spectometer (Leybold). The mass spectra showed a strong peak at the mass of the LF parent ion (256 amu) with minor contributions at 213 and 44 amu, presumably from decomposition products or CO_2. Vacuum conditions were optimized to avoid contamination of the droplets by background gas such as water or pump oil. Before each experiment the vacuum system was pumped for at least 12 h while the outer walls of the apparatus were heated to remove adsorbed water. During the experiment water was cryo-trapped by copper shields placed inside the whole flight tube with a small distance (ca. 1 cm) from the tube walls. These copper shields are cooled by connection to a liquid nitrogen reservoir. The mass spectrometer monitoring the droplet beam showed that neither water nor pump oil was transported by the beam. Since the path from the droplet source to the mass spectrometer is three times longer than the path to the LIF detection position, presence of water or pump oil inside the droplets can be excluded.

Laser induced fluorescence (LIF) was excited with a pulsed dye laser (Lambda Physics Scanmate 2E, bandwidth 0.1 cm^{-1}) pumped by the third harmonic of a Nd:YAG laser (SL803 Spectron). For excitation spectra, the emission was collected by a lens and detected with a cooled photomultiplier (R943-02, Hamamatsu), amplified (SRS 445, Stanford Research Systems), integrated by a boxcar integrator (SRS 250, Stanford Research Systems), digitized by a 12 bit A/D converter (SRS 245, Stanford Research Systems) and transmitted to a computer. A Schott GG 495 longpass transmission filter was placed before the photomultiplier in order to suppress scattered light from the dye laser.

Fluorescence spectra of LF were excited by the radiation of an Ar^+ ion laser operating in multiline UV mode. The strongest lines are at 363.8 and 333.6 nm. Fluorescence was dispersed by a spectrograph (MS257, L.O.T. Oriel, $F = 3.9$) equipped with a CCD camera (1024×255 pixel, DI 420A-BU2, Andor) Peltier cooled to −80 °C. Due to the low signal intensity the slit of the spectrograph was set to an effective spectral resolution of 15 cm^{-1}.

Quantum mechanical electronic structure calculations were performed with the GAMESS program package. For all calculations except those of the Hessian matrices for CASSCF wavefunctions the PCGAMESS implementation by A. Granovsky was used [20]. Since this version does not provide analytic second derivatives for CASSCF energies, the latter were calculated with the WinGAMESS implementation of the GAMESS-US version [21]. The 6–31G(d,p) basis set was used throughout. Excitation energies were calculated with the TD-DFT/B3LYP technique at the fixed ground state geometry optimized with DFT/B3LYP. The geometries of both electronic states S_0 and S_1 were optimized with a CAS(8,8) wavefunction. In all cases the Hessian matrix was calculated in order to verify that the stationary state is a minimum, and to obtain vibrational frequencies and normal coordinates.

3. Results and analysis

3.1. Excitation and emission spectra

The fluorescence excitation spectrum in the range 21400–23400 cm^{-1} is displayed in Fig. 1. The structural formula of lumiflavin indicating the atomic numbering scheme is shown as inset. All spectral features are assigned to He droplets containing a single lumiflavin molecule, for the following reasons: The mass spectrometer monitoring the droplet beam shows that lumiflavin is transported with the beam, but no water molecules. Water and pump oil is efficiently trapped by the liquid nitrogen cooled copper shields inside the flight tube. When water is intentionally added to the pickup cell, additional lines are seen in the spectrum, the first being 108 cm^{-1} red-shifted from the first line seen without water. When the partial pressure of the water is increased, only the new lines increase at the expense of the lines observed when no water is added to the pickup cell. If the spectrum would initially contain lines that are due to water clusters, these lines should increase when water is added.

The lowest-energy feature of the spectrum in Fig. 1 consists of a narrow line at 21511 cm^{-1} which is followed by a broader band of ca. 10 cm^{-1} width towards higher wavenumbers. The first narrow peak is by far the most intense line in the spectrum (note the axis break in Fig. 1). We assign it to the electronic origin transition 0_0^0. All other bands in the spectrum show similar widths of ca. 10 cm^{-1}. The second band is observed at 164 cm^{-1} above the origin and assigned to a mode labeled 1_0^1. This mode apparently forms progressions with the origin and with other modes. Some of these are indicated by combs (dotted lines) in Fig. 1. Although the first peak has a 3.5 times higher intensity than the second, the area under the first two bands, 0_0^0 and 1_0^1, are of comparable size. We conclude that both transitions have similar Franck–Condon factors.

Fig. 2 provides a closer look on an expanded wavenumber scale on the origin band and the first two progression bands of the low frequency mode at 164 and 327 cm^{-1}, respectively. For each band two measurements are shown, one performed with very low laser

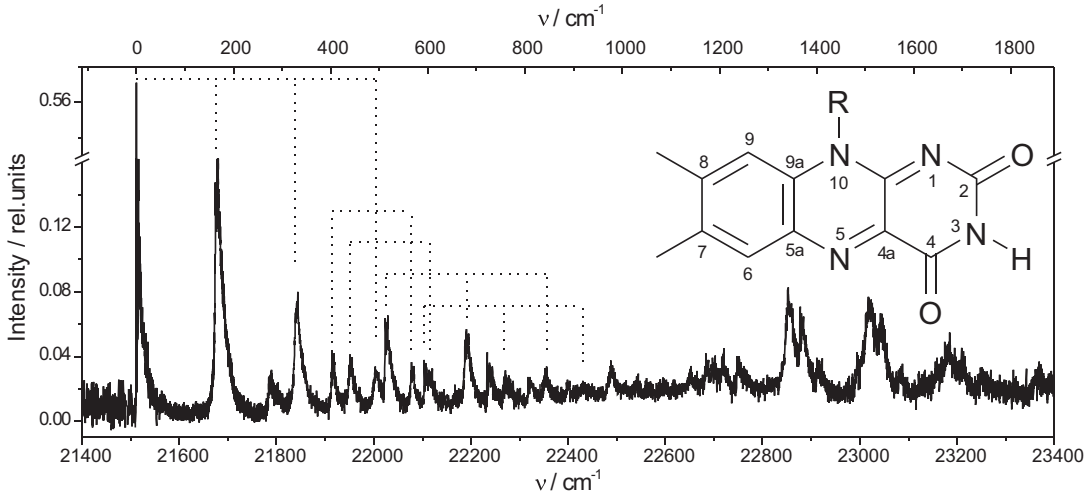

Fig. 1. Fluorescence excitation spectrum of lumiflavin isolated in superfluid He droplets. Combs of dotted lines indicate progressions in a mode with a wavenumber of 164 cm^{-1}. The structural formula and atomic numbering scheme are shown as inset.

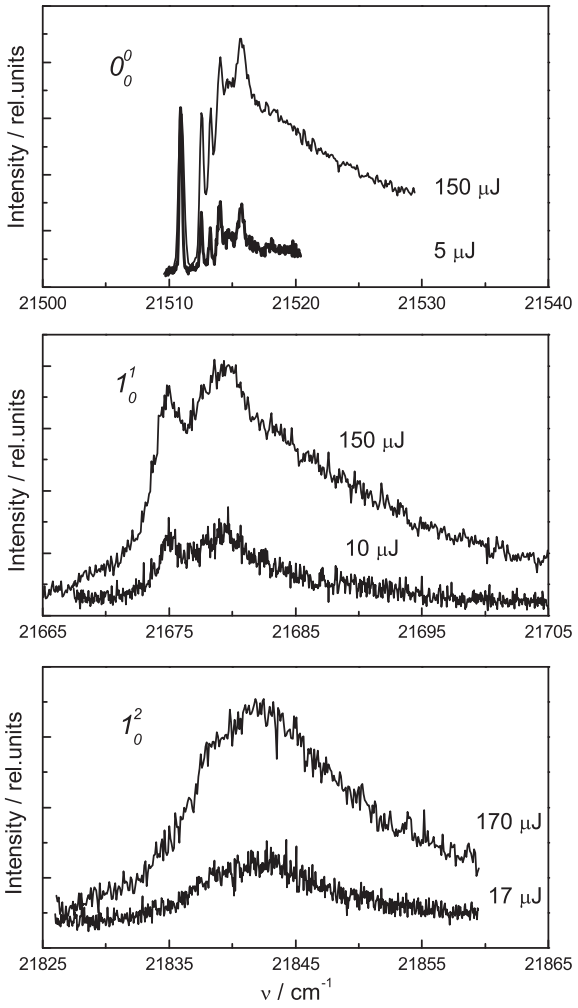

Fig. 2. Saturation behavior of the electronic origin transition 0_0^0 and the first two members 1_0^1 and 1_0^2 of the progression in the 164 cm^{-1} mode in the excitation spectrum. For each transition two spectra are shown with the laser energy per pulse indicated at each curve.

intensity (5–17 μJ/pulse), the second with much higher intensity. With increasing laser intensity the vibronic bands 1_0^1 and 1_0^2 also increase in intensity, but do not alter their shapes. The 0_0^0 band shows a different behavior. It consists of a sharp band at 21511 cm^{-1} with a width of ca. 0.5 cm^{-1} followed by weaker features extending over ca. 15 cm^{-1} with several resolved sharp peaks. When the laser intensity is increased, the shape of the first line is almost not affected, but the higher energy features gain much more in intensity and extend much further to higher wavenumbers. However, the resolved lines in the fine structure are still there. Multiplet structures within an interval of 10–15 cm^{-1} have been observed with many organic molecules doped into He droplets, mostly in the region of the electronic origin band [18,22–25]. These could be due to different sites, i.e. different arrangements of the first layer of He atoms. These are more strongly bound to the guest molecule than to the other He atoms. As a consequence they are localized and thus removed from the superfluid phase. Features on the high energy side of a zero-phonon line can also be caused by coupling of the electronic transition of the guest molecule to vibrational excitations of the He environment. This second interpretation as phonon sidebands applies more likely to the broad features: The line at 21511 cm^{-1} is the true 0_0^0 transition which has a very small homogeneous linewidth and high oscillator strength. Therefore it is easily saturated even with moderate laser intensity. Due to its much lower transition probability, the phonon sideband requires much larger laser intensities for saturation. The vibronic bands at 164 and 327 cm^{-1}, on the other side, have rather large homogeneous linewidth. The zero phonon line and the phonon sideband are barely distinguished in the 1_0^1 transition and coalesce to a single band for the 1_0^2 transition. We conclude that these vibrations relax rather quickly to the vibrationless ground state of the S_1 electronic state.

A similar observation can be made when the lineshapes of fundamental vibrational transitions are compared to those of combination bands. Fig. 3 shows the lineshapes for the electronic origin and four single quantum vibronic transitions in the left column. These are compared to the combination bands that involve, in addition to the transition in the corresponding spectrum on the left side, a further quantum in the 164 cm^{-1} mode. In the single quantum transitions on the left side the zero phonon line and the phonon sideband can be distinguished as separate bands, with the zero phonon line being considerably sharper. When this transition is combined with an additional excitation of the 164 cm^{-1} mode only a single broad band is observed.

The emission spectrum of lumiflavin doped into He droplets is shown in Fig. 4. It was excited with the two strongest UV lines of the Ar ion laser, i.e. near 27500 and 30000 cm^{-1} well above the

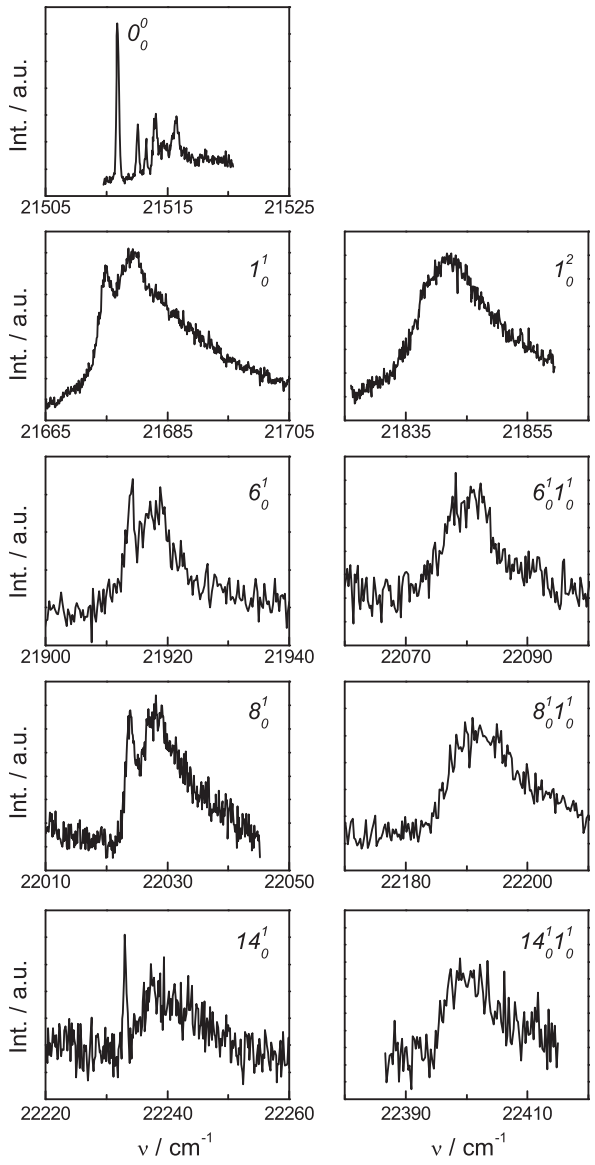

Fig. 3. Comparison of line shapes of individual fundamental modes and combination bands observed in the fluorescence excitation spectrum.

electronic origin. The highest energy feature occurs at 21511 cm^{-1}, i.e. at the same position as the line assigned to the electronic origin in the excitation spectrum. This is a manifestation of the fact that in He droplets the vibrational excess energy of vibronic excitation is quickly dissipated. This conclusion is supported by many similar observations made with many organic molecules doped into He droplets [18,22–27]. The emission spectrum thus contains no hot fluorescence band originating from vibrationally excited states in S_1, and hence the vibrational structure can be assigned to vibrations of the electronic ground state. The first three intense bands of the emission spectrum show a spacing of 164 cm^{-1}, very similar to the observation made for the excitation spectrum. We assign this to the same mode in both states and conclude that it is a totally symmetric mode with the same force constant but different equilibrium geometry in both electronic states. As indicated by the dotted combs in Fig. 4, this mode forms combinations with many other vibrations.

3.2. Assignment of vibrations

The wavenumber energies and relative intensities of all distinct vibronic lines in the excitation and emission spectra up to 1900 cm^{-1} are collected in Table 1. These vibrational shifts have been assigned to fundamental frequencies F_k by the following strategy [27–29]: For every line it was checked whether the wavenumber can, within a given tolerance, be calculated as the sum of two lines observed at lower wavenumbers. If this is not possible, the line is assigned as a fundamental wavenumber, and the relative intensity is assigned to the corresponding Franck–Condon factor. If one or more combinations are possible, the expected intensity is calculated from the Franck–Condon factors of the previously assigned modes and compared to the actual intensity of the line of interest. If the intensity of this line is much higher than any of the predicted intensities for the combinations, the line is assigned to a new fundamental. Otherwise, the line is assigned to the combination with the largest predicted intensity. This procedure was automated by a computer program. The results are displayed in columns number 4 and 7 of Table 1. In four cases two alternative assignments are given, which will be discussed later. The fundamental wavenumbers are labeled F_k for the excited state and F'_k for the ground state. Note that assignment of a fundamental frequency does not necessarily imply assignment to a normal mode. It only means that the line cannot be represented as a combination of two other lines. It might, however, correspond to a two-quantum transition in a mode for which the one-quantum transition is symmetry forbidden.

For vibrational shifts up to 1400 cm^{-1} all lines in both spectra can be represented by 11 fundamental frequencies F_1 to F_{11}. With the exception of F_7 every fundamental F_k of the excited state has a counterpart F'_k in the ground state: The pair of fundamentals has similar wavenumber and Franck–Condon factors, and forms the same combinations in both spectra. We conclude that each pair corresponds to the same normal mode. The only exception is F_7 at 722 cm^{-1} in the excited state. It can not, within the tolerance of ±5 cm^{-1}, be explained as a combination of other fundamentals. The combination $2F_1 + F_3$ is off by 8 cm^{-1}. The same applies to the combination $F_2 + F_4$, which also has a lower predicted intensity. There is no distinct line in the emission spectrum at a similar wavenumber. We conclude that the corresponding ground state vibration must have a quite different force constant. A possible candidate is the line at 837 cm^{-1}. However, this line could also be assigned as $2F'_1 + F'_5$, albeit with a mismatch of 6 cm^{-1}.

A comparison with the only other low-temperature high-resolution spectrum of a flavin available in the literature, measured in a frozen alkane matrix at 4.2 K by Platenkamp et al. [14], shows some similarities, but also differences. Seven lines are reported from the excitation spectrum with an intensity greater 7% of the origin line, namely at 156, 312, 414, 499, 514, 546, and 581 cm^{-1}. With the exception of the line at 546 cm^{-1} these can be correlated with ours at 164, 327, 403, 494, 513, and 593 cm^{-1}. Similarly, three lines with intensity greater than 7 % of the origin line in the emission spectrum in alkane matrix at 159, 323, and 596 cm^{-1} have counterparts in the He droplet spectrum at 164, 327, and 596 cm^{-1}. However, the strong lines at 39 and 517 cm^{-1} do not appear in the He droplet spectrum. Several reasons could account for these discrepancies: First, the substituent at nitrogen atom N10 in lumiflavin is a methyl group, whereas it is an undecyl group in the alkane matrix study. Vibrations whose normal coordinates strongly involve this nitrogen atom could be shifted in frequency. Also, large amplitude modes could experience a steeper effective potential in the rigid matrix compared to superfluid helium. Also, the spectra in the alkane matrix might be contaminated by contributions from other sites, e.g. by accidentally overlapping bands for the excitation frequency of the emission spectra, or the detection frequency of the excitation spectra. Another reason could be energy transfer between chromophores of different sites.

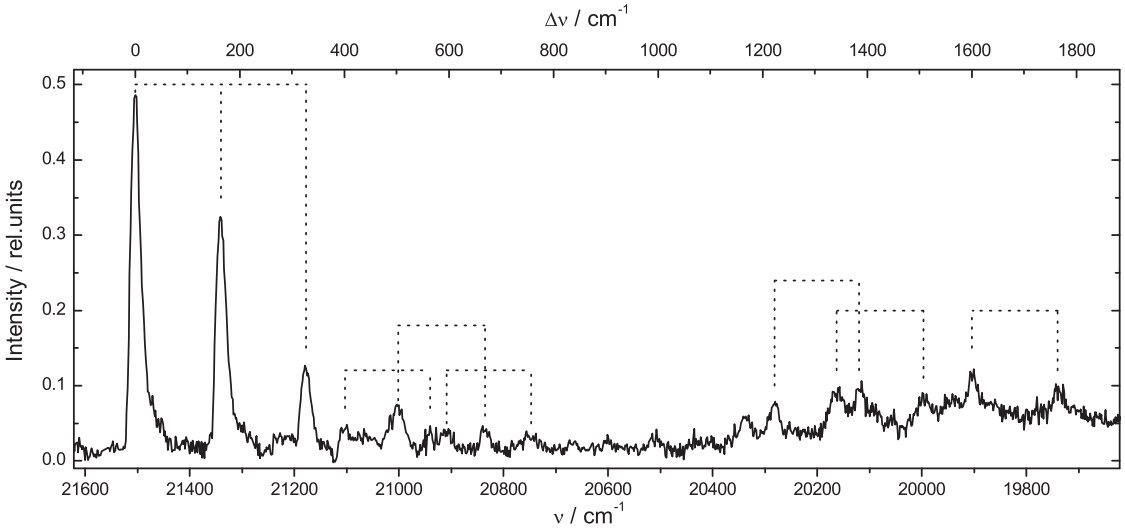

Fig. 4. Dispersed emission spectrum of lumiflavin isolated in superfluid He droplets. Combs of dotted lines indicate progressions in a mode with a wavenumber of 164 cm^{-1}.

Table 1
Positions ($\Delta\nu$) and relative intensities (I) of the lines in the excitation spectrum (left column) and the emission spectrum (right column) of LF in Helium droplets. Wavenumber shifts are given in cm^{-1} units with respect to the electronic origins at 21511 cm^{-1}. For each line an assignment in terms of a linear combination of fundamental frequencies F_k is given, followed by the mismatch in cm^{-1} units.

Line	Excitation			Emission		
	$\Delta\nu$	I	Assignment	$\Delta\nu$	I	Assignment
1	164	1.00	F_1	164	0.70	F'_1
2	274	0.19	F_2	280	0.05	F'_2
3	327	0.50	$2F_1 - 1$	327	0.25	$2F'_1 - 1$
4	403	0.25	F_3	402	0.10	F'_3
5	440	0.25	F_4	443	0.10	F'_4
6	494	0.19	$3F_1 + 2$			
7	513	0.38	F_5	503	0.20	F'_5
8	567	0.19	$F_1 + F_3$	564	0.15	$F'_1 + F'_3 - 2$
9	593	0.19	F_6	596	0.15	F'_6
10	681	0.38	$F_1 + F_5 + 4$	669	0.15	$F'_1 + F'_5 + 2$
11	722	0.25	F_7			
12	757	0.19	$F_1 + F_6$	758	0.15	$F'_1 + F'_6 - 2$
13	785	0.13	$F_2 + F_5 - 2$			
14	807	0.13	$2F_3 + 1$			
15	844	0.19	$2F_1 + F_5 + 3$	837	0.07	F'_7 or $2F'_1 + F'_5 + 6$
16	889	0.13	$F_1 + F_7 + 3$			
17	919	0.06	$F_3 + F_5 + 3$ or $2F_1 + F_6 - 2$	902	0.07	$F'_3 + F'_5 - 3$
18	978	0.25	F_8	988	0.10	F'_8
19	1029	0.19	$2F_5 + 3$			
20	1051	0.06	$2F_1 + F_7 + 1$			
21	1082	0.06	$F_1 + F_3 + F_5 + 2$			
22	1104	0.06	$F_5 + F_6 - 2$			
23	1142	0.19	$F_1 + F_8$			
24	1173	0.25	F_9	1167	0.15	F'_9
25	1205	0.25	F_{10}	1223	0.20	F'_{10}
26	1237	0.25	$F_5 + F_7 + 2$			
27	1338	0.50	F_{11}	1342	0.25	F'_{11}
28	1367	0.38	$F_1 + F_{10} - 2$	1385	0.25	$F'_1 + F'_{10} - 2$
29	1403	0.19	$F_1 + F_5 + F_7 + 4$			
30	1483	0.25	$F_1 + F_6 + F_7 + 4$			
31	1507	0.38	F_{12} or $F_1 + F_{11} + 5$	1508	0.20	$F'_1 + F'_{11} + 2$
32	1520	0.31	F_{13}			
33	1534	0.38	$2F_1 + F_{10} + 1$			
34	1573	0.19	$F_3 + F_9 - 3$	1564	0.20	F'_{12}
35	1672	0.31	$F_1 + F_{12} + 1$ or $2F_1 + F_{11} + 6$			
36	1703	0.25	$F_7 + F_8 + 3$	1600	0.20	F'_{13}
37	1740	0.19	$F_1 + F_3 + F_9$	1764	0.30	$F'_1 + F'_{13}$
38	1854	0.19	$F_1 + F_5 + F_9 + 4$			

3.3. Quantum chemical calculations

The geometry of the electronic ground state was optimized with the DFT/B3LYP method. This method yields usually structures and vibrational frequencies in good agreement with experiment. For consistency we use this geometry for the calculation of electronic excitation energies by the TD-DFT method. Excitation energies calculated by TD-DFT converge much faster with increasing basis sets compared to methods using configuration interaction, as has been particularly shown for flavins by Neiss et al. [30]. Our excitation energies, shown in Table 2, are in good agreement with those previously obtained with similar basis sets [30–33]. In particular, we find the lowest excited A′($\pi\pi^*$) state at ca. 400 cm^{-1} lower energy than the lowest A″ ($n\pi^*$) state.

For a comparison of the vibrational frequencies in the S_0 and S_1 electronic states we used CASSCF(8,8) wavefunctions for both states in order to generate data of similar quality. The optimized structures for these two states are shown in Fig. 5 and compared to the structure calculated for the S_0 state with DFT. A comparison of the two geometries for the electronic ground state shows that DFT calculates systematically longer bond lengths, in particular for all C–H, N–H, and C=O bonds. When CASSCF finds a longer bond, the difference is always less than 1 pm.

The differences between the two CASSCF structures for S_0 and S_1 are larger. The greatest changes occur for the lengths of bond C5–C5a, which decreases by 5 pm upon electronic excitation, and the bonds C4a–N5 and C6–C7, which increase by 7 pm and 8 pm,

Table 2
Transition energies and oscillator strength f calculated by the TD-DFT method for the vertical transitions originating from the electronic ground state of LF.

State	TD-DFT			
	ΔE/eV	$\Delta\nu/cm^{-1}$	λ/nm	f
2A′	3.0371	24496	408.24	0.1916
1A″	3.0850	24882	401.89	0.0003
2A″	3.2957	26581	376.20	0.0006
3A″	3.8407	30977	322.82	0.0000
3A′	3.8596	31130	321.24	0.1335
4A′	4.0018	32277	309.82	0.0112
4A″	4.6225	37283	268.22	0.0003
5A′	4.7118	38003	263.14	0.0707
6A′	4.9105	39606	252.49	0.5910
5A″	4.9624	40025	249.85	0.0000

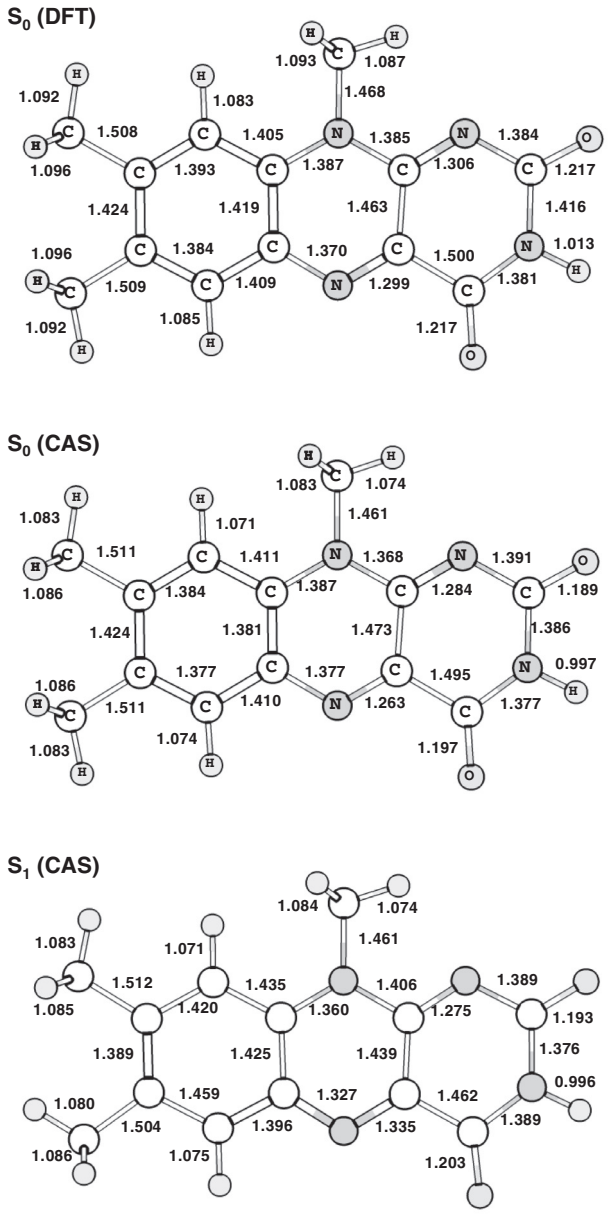

Fig. 5. Structures indicating optimized bond lengths of the electronic ground state S_0 and the first electronically excited state S_1 of lumiflavin. Both states were optimized in C_S symmetry with a CASSCF(8,8)/6–31G(d,p) wavefunction. The ground state was also optimized with the DFT/6–31G(d,p) method.

respectively. Also, the methyl group on C7 rotates by 60°, assuming a staggered configuration with respect to the methyl group on C8. The eclipsed configuration, which is the minimum in S_0, is a transition state in S_1. Such a shift of the potential minima for a hindered rotor has the consequence that each hindered rotor state in each electronic state has substantial Franck–Condon factors with the rotor states of the other electronic state. High resolution spectra of such molecules measured, e.g., in supersonic jets show progressions in this hindered rotor mode which are usually strongly anharmonic. In He nanodroplets these rotor modes are strongly damped and the spectra can be modeled by convolution of the jet spectra with a Lorentzian lineshape [34]. Hence this mechanism may also contribute to the broadening observed in the excitation and emission spectra of LF in helium droplets.

Table 3
Calculated vibrational wavenumbers for the S_0 and S_1 states.

S_0				S_1			
$\Delta\nu$	Sym	$\Delta\nu$	Sym	$\Delta\nu$	Sym	$\Delta\nu$	Sym
173.4	1a′	37.9	1a″	172.3	1a′	40.5	1a″
297.2	2a′	65.4	2a″	289.2	2a′	50.0	2a″
313.7	3a′	101.3	3a″	304.5	3a′	66.3	3a″
344.5	4a′	122.4	4a″	344.7	4a′	91.2	4a″
378.5	5a′	127.8	5a″	374.5	5a′	128.5	5a″
432.6	6a′	149.5	6a″	430.3	6a′	137.6	6a″
473.0	7a′	177.6	7a″	473.9	7a′	167.5	7a″
536.4	8a′	198.1	8a″	533.3	8a′	170.7	8a″
548.5	9a′	213.1	9a″	551.0	9a′	211.0	9a″
578.7	10a′	257.1	10a″	578.1	10a′	223.1	10a″
644.8	11a′	349.3	11a″	642.2	11a′	313.1	11a″
681.3	12a′	388.9	12a″	656.4	12a′	342.4	12a″
726.2	13a′	471.3	13a″	722.3	13a′	380.8	13a″
788.3	14a′	551.3	14a″	760.0	14a′	457.4	14a″
850.5	15a′	646.5	15a″	832.3	15a′	562.1	15a″
894.0	16a′	680.6	16a″	884.2	16a′	667.5	16a″
923.6	17a′	720.8	17a″	922.4	17a′	695.7	17a″
1057.1	18a′	804.6	18a″	1053.2	18a′	720.3	18a″
1095.8	19a′	838.3	19a″	1063.4	19a′	762.1	19a″
1108.3	20a′	849.3	20a″	1083.5	20a′	811.5	20a″
1122.8	21a′	913.9	21a″	1109.6	21a′	871.9	21a″
1162.9	22a′	952.5	22a″	1155.5	22a′	890.5	22a″
1192.9	23a′	1132.5	23a″	1233.1	23a′	1110.6	23a″
1248.9	24a′	1148.6	24a″	1272.9	24a′	1133.4	24a″
1303.5	25a′	1253.7	25a″	1298.8	25a′	1253.0	25a″
1344.6	26a′	1607.4	26a″	1313.6	26a′	1606.9	26a″
1359.3	27a′	1623.3	27a″	1332.9	27a′	1623.2	27a″
1397.1	28a′	1644.5	28a″	1374.2	28a′	1646.4	28a″
1421.0	29a′	3242.7	29a″	1420.5	29a′	3239.9	29a″
1468.7	30a′	3249.5	30a″	1442.1	30a′	3254.2	30a″
1488.6	31a′	3278.8	31a″	1465.4	31a′	3264.6	31a″
1543.3	32a′			1542.5	32a′		
1547.9	33a′			1551.9	33a′		
1560.8	34a′			1560.0	34a′		
1565.0	35a′			1561.2	35a′		
1574.4	36a′			1582.5	36a′		
1595.3	37a′			1597.0	37a′		
1614.9	38a′			1615.1	38a′		
1623.3	39a′			1630.4	39a′		
1639.9	40a′			1633.5	40a′		
1651.0	41a′			1649.9	41a′		
1732.4	42a′			1657.8	42a′		
1766.9	43a′			1673.3	43a′		
1793.8	44a′			1741.6	44a′		
1864.2	45a′			1812.4	45a′		
1978.0	46a′			1940.8	46a′		
2013.4	47a′			1992.7	47a′		
3186.8	48a′			3186.8	48a′		
3191.8	49a′			3193.1	49a′		
3211.8	50a′			3200.6	50a′		
3272.3	51a′			3271.2	51a′		
3274.9	52a′			3306.7	52a′		
3374.3	53a′			3379.5	53a′		
3379.9	54a′			3384.4	54a′		
3400.8	55a′			3413.0	55a′		
3862.7	56a′			3875.0	56a′		

4. Discussion

We assign the excitation spectrum and the emission spectrum observed in this work to transitions between the S_0 and $S_1(\pi\pi^*)$ electronic states of lumiflavin. This is in line with our own as well as earlier TD-DFT calculations by others [30–33]. The lowest $n\pi^*$ transition is calculated at ca. 400 cm^{-1} higher energy (see Table 2), also in agreement with Ref. [30–33]. The calculated intensity is three orders of magnitude below that for the $\pi\pi^*$ transition. In a condensed medium a $\pi\pi^*$ transition will experience a stronger red shift than a $n\pi^*$ transition.

As far as we know, the first normal mode analysis for lumiflavin was presented by Bowman and Spiro [35]. It was restricted to

Table 4
Comparison of fundamental vibrational wavenumbers (in cm^{-1} units) for the S_1 state (obtained from the fluorescence excitation spectra) and for the S_0 state (obtained from the dispersed fluorescence spectra) with CASSCF calculations for these electronic states. Calculated values are scaled by a factor of 0.933.

Raman		He droplet		CASSCF (8,8)		Label
Ref. [40]	Ref. [45]	S_0	S_1	S_0	S_1	
		164	164	162	161	1a′
		280	274	293	284	3a′
		402	403	404	401	6a′
429	418	443	440	441	442	7a′
521	527	503	513	500	498	8a′
605	608	596	593	602	599	11a′
740	741		722	735	709	14a′
994	993	988	978	986	983	18a′
1157	1150	1167	1173	1165	1188	24a′
1256	1243	1223	1205	1216	1212	25a′
		1342	1338	1326	1325	29a′

in-plane vibrations, and the empirical force field was not optimized, so that calculated and experimental wavenumbers of the vibrations in the S_0 potential differed by as much as 100 cm^{-1}. A later analysis by Abe and Kyogoku [36] used an optimized force field and the Wilson GF matrix method, resulting in good agreement for the Raman and IR lines of LF and several isotopically substituted compounds. In 1990 Lively and McFarland published yet another normal mode analysis [37] based on the semiempirical QCFF-π method developed by Warshel and Karplus [38,39]. This method determines the contribution of the π-electron system to the force field by a semiempirical quantum mechanical calculation. This study presents also out-of-plane (oop) motions, and reassigns in particular two low-frequency vibrations (i.e. Raman lines at 429 and 605 cm^{-1} [40]) to oop modes.

All three studies calculated vibrations in the spectral range below 400 cm^{-1}, but at that time no corresponding data were available from IR or Raman experiments. Abe and Kyogoku [36] find six in-plane modes in this range, at wavenumbers of 148, 218, 228, 289, 304, and 388 cm^{-1}. With the exception of the first one, all of these have contributions of the bending coordinates of the three methyl groups. Lively and McFarland [37] list 17 modes in this spectral region, but they present only the frequencies and do not discuss them.

The dramatic progress in computer technology and quantum chemical algorithm in the last two decades now permits the calculation of ab initio force fields for larger molecules not only for the electronic ground state, but also for excited states. Several such studies dealing with the flavin chromophore have been published recently [41–44]. The first three use Hartree Fock and DFT wavefunctions for the electronic ground state, and CIS wavefunctions for the first electronically excited state. Klaumünzer et al. use TD-DFT. Unfortunately for us, all of these studies concentrate on effects of solvent or protein environment, and ultrafast dynamics, but are not interested in vibrations below ca. 1300 cm^{-1}. Although such vibrations were certainly produced by these calculations, the authors do not discuss them. However, Klaumünzer et al. present calculations on the vibronic absorption and emission spectra which apparently include all the vibrations in both electronic states [44]. In this simulated absorption spectrum (Fig. 5 in their paper), the most intense line besides the electronic origin is labeled as an in-plane vibration with a shift of ca. 4 nm (ca. 190 cm^{-1}) from

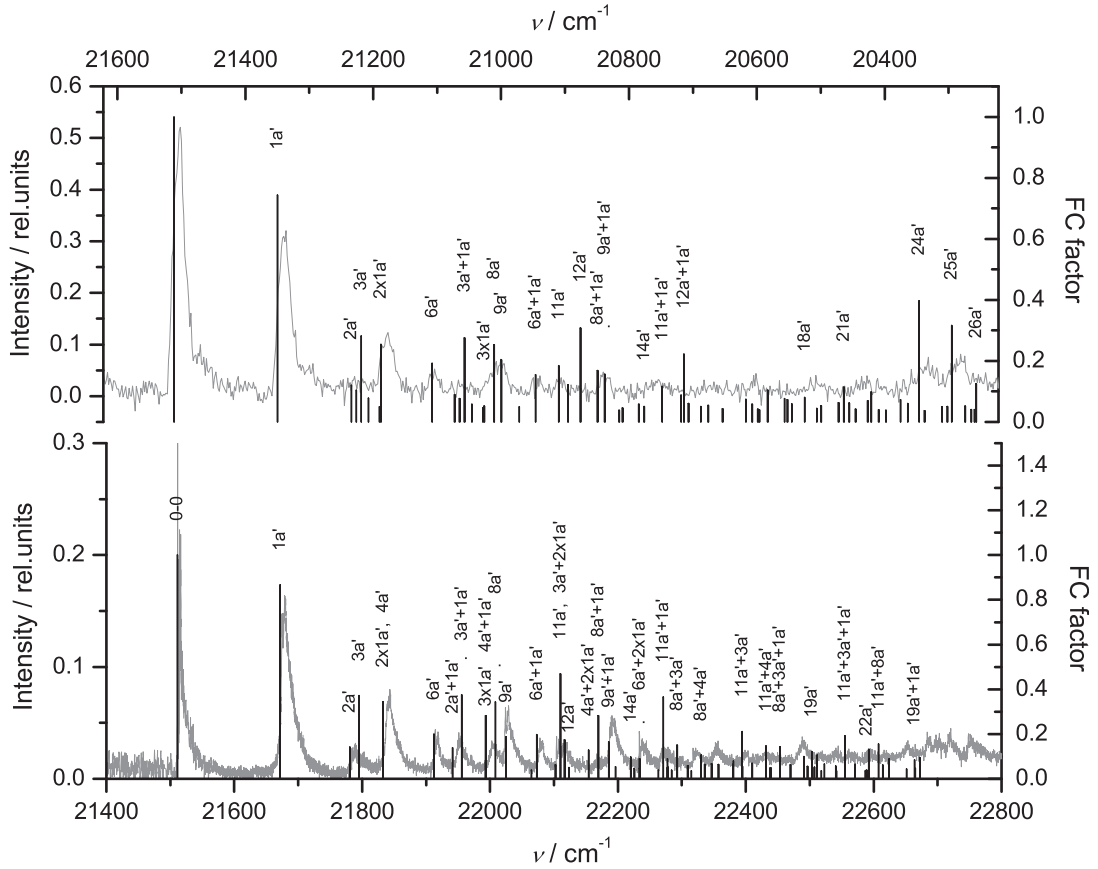

Fig. 6. Franck–Condon pattern of the excitation and emission spectra, calculated with the optimized geometries and ab initio force fields from CASSCF calculations on S_0 and S_1. The experimental spectra are shown as dotted lines. Labels indicate assignment in terms of the vibrations listed in Table 3.

the electronic origin. This is in good agreement with our experimental finding of a strong progression forming mode of 164 cm^{-1}.

Since we could not find vibrational frequencies in the spectral range relevant to our experiments from published quantum chemical calculations, we performed geometry optimizations with CASSCF(8,8)/6–31G(d,p) wavefunctions for the lowest two A′ states of lumiflavin, followed by calculation of the Hessian and vibrational frequencies. Although DFT might yield better agreement for the vibrations of the electronic ground state, the use of the same method for both electronic states should yield data of the same quality which may be compared. The results are collected in Table 3. These frequencies were then scaled by a common factor of 0.933. Table 4 compares the fundamental frequencies F_1 – F_{11} extracted from the analysis of the dispersed fluorescence (DF) and the laser induced fluorescence (LIF) spectra with scaled normal mode frequencies from the calculations for S_0 and S_1. Two additional columns in this table list ground state frequencies from Raman measurements [45,40]. Each experimental frequency can be assigned to an in-plane vibration. Apparently, most of these frequencies do not change much upon electronic excitation, both in experiment and in theory. An exception is the mode at 722 cm^{-1} in the excitation spectrum which does not show a counterpart in emission. The calculated frequencies of the corresponding mode 14a′ in the S_0 and S_1 states differ by only 4%.

Since a comparison solely based on the values of the vibrational wavenumbers could produce accidental coincidences, in particular when the number of vibrations is large, we also performed calculations of the Franck–Condon factors for the $S_0 \rightarrow S_1$ excitation spectrum and the $S_1 \rightarrow S_0$ emission spectrum. We used the program Momo-fcf developed by Momose et al. [46] based on the recursion relations developed by Kupka and Cribb [47]. The program uses the optimized geometries and normal modes from the CASSCF calculations of both states. The only modification was a common scaling of all vibrational frequencies by a factor of 0.933. The calculation was performed for a temperature of 0 K, i.e. the initial state was restricted to the zero vibrational state. The line positions and intensities for all transitions up to a total vibrational energy of 1344 cm^{-1} (unscaled) were calculated and are shown as vertical bars in Fig. 6, superimposed on the experimental spectra. For the most intense lines the vibrational states involved are indicated by the same symmetry label used in Table 3.

The strongest progression forming mode is obviously 1a′ in both electronic transitions, in very good agreement with experiment. The normal coordinate of this mode is shown in Fig. 7. It is very similar in both electronic states and involves mostly a synchroneous in-plane bending of the two methyl groups at ring I of the flavin. The calculation also finds considerable intensity for the modes 3a′, 4a′, 6a′, 8a′, 9a′, and 11a′ in the excitation spectrum, and for 3a′, 6a′, 8a′, 9a′, 11a′, 12a′, 24a′, and 25a′ in the dispersed emission spectrum. Most of the calculated lines are close to a line with similar intensity in the corresponding spectrum, with the exception of 3a′ and 12a′ in emission and 3a′ and 11a′ in excitation.

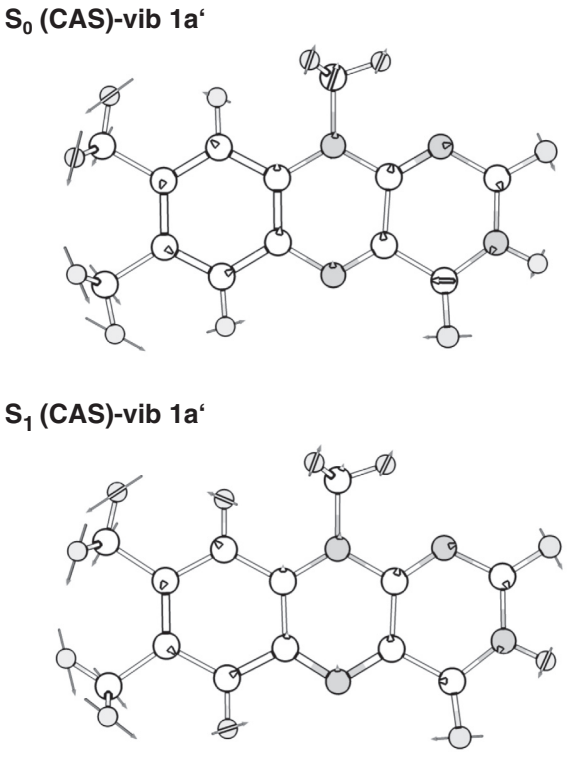

Fig. 7. Normal coordinate of the strongest progression forming mode 1a′ at 164 cm^{-1} in the S_0 and the S_1 states.

5. Summary

Individual lumiflavin molecules have been incorporated into superfluid He nanodroplets and cooled to 370 mK. The fluorescence excitation and dispersed emission spectra of these molecules are assigned to the transition between the electronic ground state and the first electronically excited singelt state of $\pi\pi^*$ character. The rich vibrational structure up to ca. 1800 cm^{-1} in both spectra can be analyzed in terms of only 13 fundamental frequencies. A prominent mode of 164 cm^{-1} produces progressions in both spectra. The corresponding normal coordinate, mostly an in-plane bending of the whole isoalloxazine system with large amplitudes on the two methyl groups of flavin ring I, has a large overlap with the vector describing the geometrical change upon electronic excitation. Multidimensional Franck–Condon factors calculated with the CASSCF optimized geometries and harmonic force fields are in good agreement with the low-energy part of both spectra.

Acknowledgments

AV acknowledges a postdoctoral stipend by the German Science Foundation (Deutsche Forschungsgemeinschaft) in the framework of the Research Training Group (GRK-640) Sensory Photoreceptors.

References

[1] M.A. van der Horst, K.J. Hellingwerf, Acc. Chem. Res. 37 (2004) 13.
[2] S. Crosson, S. Rajagopal, K. Moffat, Biochemistry 42 (2003) 2.
[3] W.R. Briggs, J. Biomed. Sci. 14 (2007) 499.
[4] A. Losi, Photochem. Photobiol. 83 (2007) 1283.
[5] M. Gomelsky, G. Klug, Trends Biochem. Sci. 27 (2002) 497.
[6] M. Gomelsky, W.D. Hoff, Trends Microbiol. 19 (2011) 441.
[7] A. Batschauer, R. Banerjee, R. Pokorny, Annu. Plant Rev. 30 (2007) 17.
[8] I. Chaves, R. Pokorny, M. Byrdin, N. Hoang, T. Ritz, K. Brettel, L.-O. Essen, G.T.J. van, der Horst, A. Batschauer, M. Ahmad, Annu. Rev. Plant Biol. 62 (2011) 335.
[9] A. Sancar, Adv. Electron Trans. Chem. 2 (1992) 215.
[10] L.O. Essen, T. Klar, Cell. Mol. Life Sci. 63 (2006) 1266.
[11] A. Weigel, A. Dobryakov, B. Klaumunzer, M. Sajadi, P. Saalfrank, N.P. Ernsting, J. Phys. Chem. B 115 (2011) 3656.
[12] B. Rieff, S. Bauer, G. Mathias, P. Tavan, J. Phys. Chem. B 115 (2011) 2117.
[13] J.P. Gotze, C. Greco, R. Mitric, V. Bonacic-Koutecky, P. Saalfrank, J. Comput. Chem. (2012).
[14] R.J. Platenkamp, H.D. Van Osnabrugge, A.J.W.G. Visser, Chem. Phys. Lett. 72 (1980) 104.
[15] J.P. Toennies, A.F. Vilesov, Angew. Chem. Int. Ed. 43 (2004) 2622.
[16] A. Slenczka, J.P. Toennies, Chemical dynamics inside superfluid helium nanodroplets at 0.37 K, in: Low Temperatures And Cold Molecules, Imperial College Press, 2008, pp. 345–392.
[17] A. Slenczka, B. Dick, M. Hartmann, J. Peter, J. Chem. Phys. 115 (2001) 10199.
[18] R. Lehnig, A. Slenczka, J. Chem. Phys. 118 (2003) 8256.
[19] R.M. Cresswell, T. Neilson, H.C.S. Wood, J. Chem. Soc. (1961) 4776.
[20] A. Granovsky. <http://www.classic.chem.msu.su/gran/firefly/index.html>.

[21] A precompiled version for use on windows computers can be downloaded from: <http://www.msg.chem.iastate.edu/GAMESS/GAMESS.html>.
[22] R. Lehnig, A. Slenczka, J. Chem. Phys. 120 (2004) 5064.
[23] R. Lehnig, A. Slenczka, Chem. Phys. Chem. 5 (2004) 1014.
[24] R. Lehnig, A. Slenczka, J. Chem. Phys. 122 (2005) 244317/1.
[25] D. Pentlehner, A. Slenczka, Mol. Phys. 110 (2012) 1933.
[26] R. Lehnig, D. Pentlehner, A. Vdovin, B. Dick, A. Slenczka, J. Chem. Phys. 131 (2009) 194307/1.
[27] A. Stromeck-Faderl, D. Pentlehner, U. Kensy, B. Dick, Chem. Phys. Chem. 12 (2011) 1969.
[28] R. Seiler, B. Dick, Angew. Chem. Int. Ed. 40 (2001) 4020.
[29] R. Seiler, U. Kensy, B. Dick, Phys. Chem. Chem. Phys. 3 (2001) 5373.
[30] C. Neiss, P. Saalfrank, M. Parac, S. Grimme, J. Phys. Chem. A 107 (2003) 140.
[31] E. Sikorska, I.V. Khmelinskii, J. Koput, M. Sikorski, J. Molec. Struct. Theochem. 676 (2004) 155.
[32] K. Zenichowski, M. Gothe, P. Saalfrank, J. Photochem. Photobiol. A 190 (2007) 290.
[33] S. Salzmann, J. Tatchen, C.M. Marian, J. Photochem. Photobiol. A 198 (2008) 221.
[34] D. Pentlehner, C. Greil, B. Dick, A. Slenczka, J. Chem. Phys. 133 (2010) 114505/1.
[35] W.D. Bowman, T.G. Spiro, Biochemistry 20 (1981) 3313.
[36] M. Abe, Y. Kyogoku, Spectrochim. Acta Part A 43A (1987) 1027.
[37] C.R. Lively, J.T. McFarland, J. Phys. Chem. 94 (1990) 3980.
[38] A. Warshel, M. Karplus, J. Am. Chem. Soc. 94 (1972) 5612.
[39] A. Warshel, M. Karplus, Chem. Phys. Lett. 17 (1972) 7.
[40] R.A. Copeland, T.G. Spiro, J. Phys. Chem. 90 (1986) 6648.
[41] M.M.N. Wolf, C. Schumann, R. Gross, T. Domratcheva, R. Diller, J. Phys. Chem. B 112 (2008) 13424.
[42] M.T.A. Alexandre, T. Domratcheva, C. Bonetti, L.J.G.W. van Wilderen, R. van Grondelle, M.-L. Groot, K.J. Hellingwerf, J.T.M. Kennis, Biophys. J. 97 (2009) 227.
[43] M.M.N. Wolf, H. Zimmermann, R. Diller, T. Domratcheva, J. Phys. Chem. B 115 (2011) 7621.
[44] B. Klaumunzer, D. Kroner, P. Saalfrank, J. Phys. Chem. B 114 (2010) 10826.
[45] Y. Nishina, K. Shiga, K. Horiike, H. Tojo, S. Kasai, K. Yanase, K. Matsui, H. Watari, T. Yamano, J. Biochem. (Tokyo) 88 (1980) 403.
[46] M. Yamaguchi, T. Momose, T. Shida, J. Chem. Phys. 93 (1990) 4223.
[47] H. Kupka, P.H. Cribb, J. Chem. Phys. 85 (1986) 1303.